Transition-State Stabilization and Enzymic Catalysis. Kinetic and Molecular Orbital Studies of the Rearrangement of Chorismate to Prephenate†

P. R. Andrews, Geoffrey D. Smith,* and I. G. Young

ABSTRACT: The nonenzymatic conversion of chorismate to prephenate has been studied to provide information relevant to the mechanism of the enzyme-catalyzed reaction. Kinetic studies show that between 20 and 65° chorismate is approximately 80% converted to prephenate and thence phenylpyruvate in a consecutive reaction and 20% converted to other products (mainly 4-hydroxybenzoate). By measuring the temperature dependence of the rates of these reactions we have shown that the first-order rearrangement of chorismate to prephenate has an enthalpy of activation of 20.71 ± 0.35 kcal/mol and an entropy of activation of −12.85 ± 0.42 eu. Using the turnover number calculated from the maximum velocity of the enzymatic reaction with chorismate mutase–prephenate dehydrogenase from *Aerobacter aerogenes* (Koch, G. L. E., Shaw, D. C., and Gibson, F. (1970), *Biochim. Biophys. Acta 212*, 375; (1972), *ibid. 258*, 719) we have calculated that this enzyme enhances the rate of reaction at pH 7.5 and 37° by a factor of 1.9×10^6. Depending on the influence of the enzyme on the entropy of activation this corresponds to a reduction in the enthalpy of activation of 4.9–8.9 kcal/mol which may be ascribed to stabilization of the transition state by bond formation to the active site. Molecular orbital calculations with extended Hückel theory were used to determine the most stable conformations of chorismate, prephenate, and the transition state. The calculations show that prephenate is favored by 1.5 kcal/mol over chorismate and that the equatorial form (with respect to the oxygen functions) of the hexadiene ring of chorismate is 7 kcal/mol more stable than the axial form, which is essentially the structure determined for the ring in the transition state. Assuming the transition-state structure to be a reflection of the active site of the enzyme, these calculations allow speculation concerning the nature of the bonds important for transition-state stabilization.

Enzymes are thought to achieve their enormous rate enhancements of biological reactions in two main ways: (i) a reduction in the entropy difference between the substrate(s) and the transition state which results from the greater loss of entropy by the substrate(s) on binding to the enzyme. This effect has also been described wholly or partly as a proximity, concentration, or orbital steering effect (Page and Jencks, 1971; Dafforn and Koshland, 1971; Page, 1972); (ii) a reduction in the enthalpy difference between the substrate(s) and the transition state when both are bound to the enzyme. This results from the greater affinity of the transition state for the active site of the enzyme. This effect has also been described as a strain or distortion effect (Jencks, 1969).

In the case of intramolecular reactions the problem is greatly simplified because the entropy effect involves only the loss of internal rotational freedom and a study of the activity of the enzyme reduces largely to a consideration of bond formation favoring the transition state over the substrate. A particularly interesting enzymatic reaction in this class is the intramolecular rearrangement of chorismate to prephenate, which is the first specific step in the biosynthetic pathways leading to tyrosine and phenylalanine in bacteria and other organisms (see Gibson and Pittard, 1968). This reaction also proceeds spontaneously in *vitro*, probably by an Sni′ mechanism (see Edwards and Jackman, 1965). We have studied this nonenzymatic conversion of chorismate to prephenate in order to provide information relevant to the mechanism of the enzyme-catalyzed reaction.

We have measured the temperature dependence of the rate of the nonenzymatic conversion and have thus obtained the enthalpy and entropy of activation for this reaction. These data, together with the calculated turnover number for the enzymatic reaction, provide a quantitative estimate of the reduction in enthalpy of activation resulting from the interaction between the active site and the transition state. We have then deduced the likely structure of the transition state and other relevant species by computing a multidimensional potential energy surface for the reaction using molecular orbital theory. The combination of kinetic and molecular orbital data thus provides a basis for speculation on the nature and function of the active site.

Experimental Section

Materials and Methods

Chorismic acid, prepared by the method of Gibson (1970), was kindly donated by J. Lawrence.

For the determination of the rates of conversion of chorismate to prephenate and phenylpyruvate, a solution of chorismate (approximately 1 mM) was prepared by dissolving the solid compound in buffer (0.02 M Tris-HCl, pH 7.5 at 20°) which had been preequilibrated at the appropriate temperature in a waterbath accurate to ±0.01°. At various times after dissolution three aliquots (0.5 ml) were withdrawn for the estimation of chorismate, prephenate and phenylpyruvate concentrations.

Chorismate concentrations were determined by quantitative conversion to anthranilate using a cell extract of the *Aerobacter aerogenes* mutant 62-1 (Gibson and Gibson, 1964). This strain, which lacks chorismate mutase–prephenate dehydratase (EC 4.2.1.51), chorismate mutase–prephenate dehydrogenase (EC 1.3.1.12), and indole glycerol phosphate

† From the Departments of Physical Biochemistry and Biochemistry, The John Curtin School of Medical Research, Australian National University, Canberra, Australia, 2601. *Received March 19, 1973.*

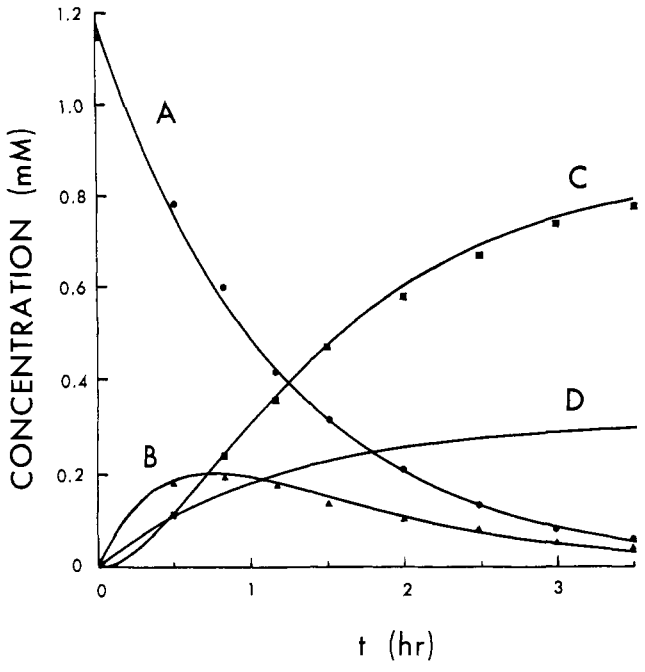

FIGURE 1: Experimental and simulated kinetic data for the conversion of chorismate to other products at 55.3°. Chorismate (A, ●), prephenate (B, ▲), and phenylpyruvate (C, ■) concentrations were determined as described in the Experimental Section. The solid lines are simulated curves for the reactions based on the scheme of eq 1, using the experimentally determined values of k_1 (1.781×10^{-4} sec^{-1}), k_2 (5.399×10^{-4} sec^{-1}), and k_3 (6.455×10^{-5} sec^{-1}). The curve for compound(s) D was obtained by difference.

synthase (EC 4.1.1.48), was grown on limiting indole to derepress anthranilate synthase (EC 4.1.3.27) and the cell extract was prepared (Egan and Gibson, 1972) in Tris buffer (0.05 M Tris-HCl, pH 7.5). An aliquot (0.5 ml) from the reaction mixture was added to 0.2 ml of a solution containing magnesium chloride (50 mM) and glutamine (25 mM) in 0.02 M Tris-HCl (pH 7.5) and 0.2 ml of the *A. aerogenes* 62-1 extract (containing about 25 mg of protein/ml) preequilibrated at 37°. Under these conditions a 1 mM solution of chorismate was more than 90% converted to anthranilate in 5 min and conversion was essentially complete after 25 min, at which time 1 N HCl (0.1 ml) was added and the solution was extracted with ethyl acetate (4 ml). The extract was then dried with Na_2SO_4 and the optical density at 336 nm was read against an appropriate blank. A standard curve for anthranilate was constructed similarly.

Prephenate concentrations were determined by conversion to phenylpyruvate under acid conditions using the method described by Gibson and Gibson (1964). The increase in optical density at 320 nm of the blanks (read against water) used in these assays was taken as a measure of the rate of phenylpyruvate formation in the reaction mixture itself.

Molecular Orbital Calculations. The molecular orbital calculations were carried out using extended Hückel theory (EHT), which was developed by Hoffman (1963) to provide a simple treatment of all valence electrons in molecules which are not fully conjugated. Although the method is essentially empirical, it may be derived from rigorous self-consistent field theory by applying relatively minor approximations (Blyholder and Coulson, 1968), and the EHT calculation of total energy has been specifically rationalized (Allen and Russell, 1967). Accordingly, EHT has been successfully applied to several conformational problems of biological interest (Kier, 1972). Calculations were executed for various conformations of chorismate, prephenate, and intermediate structures using the computer program and parameters described previously by Andrews (1969). Except for slight adjustments for ring closure, standard bond lengths and angles (Sutton, 1965) were employed for the chorismate and prephenate geometries and interpolated values were derived for transition species. Dihedral angles describing possible molecular conformations were generally incremented by 60° and energies were calculated for all conformations not excluded by unreasonably short interatomic bond distances. For some conformational variables increments of less than 60° were necessary before an unambiguous contour map could be obtained, but the minimum increment used was 10°.

TABLE I: Rate Constants for the Conversion of Chorismate to Other Products at Different Temperatures.[a]

T (°C)	$k_1 \times 10^5$ (sec^{-1})	$k_2 \times 10^5$ (sec^{-1})	$k_3 \times 10^6$ (sec^{-1})
21.8	0.407	0.0431	1.208
29.9	1.235	0.362	1.388
36.9	2.598	1.048	4.159
45.0	6.428	8.009	7.862
55.3	17.81	53.99	64.55
64.6	42.68	250.8	152.3

[a] The rate constants are those measured for the reactions shown schematically in eq 1. The method of their calculation is described in the text.

Results

Experimental Results. The variation in concentration of chorismate, prephenate, and phenylpyruvate with time at 55.3° is illustrated in Figure 1. These data are representative of those at all temperatures studied and have been interpreted in terms of the scheme

$$\begin{array}{ccccc} A & \xrightarrow{k_1} & B & \xrightarrow[[H^+]]{k_2} & C \\ \downarrow{\scriptstyle k_3} & & & & \\ D & & & & \end{array} \qquad (1)$$

where A, B, and C represent chorismate (Figure 4), prephenate (Figure 6) and phenylpyruvate, respectively, and D represents other products, presumed to be largely or wholly 4-hydroxybenzoate (Young *et al.*, 1969). The rate constants k_1 and k_3 are first-order, with k_3 being either a single rate constant or the sum of separate first-order constants, depending on how many products are represented by D, and k_2 is the rate constant for the acid hydrolysis, B → C (Gilvarg, 1955). Since the pH must remain constant at any particular temperature this reaction behaves as pseudo-first-order.

At each temperature k_1 was obtained (Table I) by a least-squares analysis of the data according to the linear equation

$$\ln c_A = -\frac{dc_A}{d(c_B + c_C)} k_1 t + \ln c_0 \qquad (2)$$

where c_A, c_B, and c_C are the molar concentrations of A, B, and C at time t, and c_0 is the concentration of A at the initial

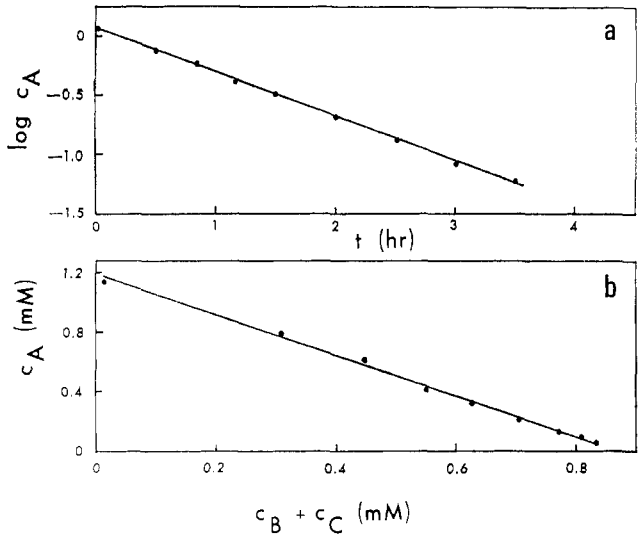

FIGURE 2: Plots obtained at 55.3° for the first-order decomposition of chorismate. In part a is shown the log of the chorismate concentration (mM) as a function of time and in part b is a plot of chorismate concentration, c_A *vs.* the sum of the concentrations of prephenate (c_B) and phenylpyruvate (c_C) for the same time period.

time. A plot of log c_A *vs.* t at 55.3° is given in Figure 2a. The term $dc_A/d(c_B + c_C)$ and hence the fraction of chorismate which has been converted to prephenate in a given time interval was obtained from plots of c_A *vs.* $(c_B + c_C)$. The linearity of these plots (*e.g.*, Figure 2b) is consistent with the assumption that k_3 is first order and that phenylpyruvate is the sole product from prephenate under the conditions used. The proportion of chorismate converted to prephenate appeared to be effectively independent of temperature, and was found to be 81 ± 8%. Values of k_3 were obtained by difference (Table I).

An average value of k_2 was obtained at each temperature by numerically solving the equation

$$c_B = c_0 \frac{k_1}{k_2 - k_1 - k_3}[e^{-(k_1 + k_3)t} - e^{-k_2 t}] \qquad (3)$$

at different times. Equation 3 was derived by an extension of the method of Glasstone and Lewis (1961). Values of k_2 are tabulated in Table I.

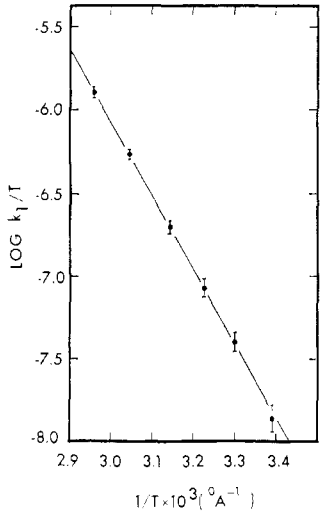

FIGURE 3: Temperature dependence of k_1, the first-order rate constant describing the conversion of chorismate to prephenate.

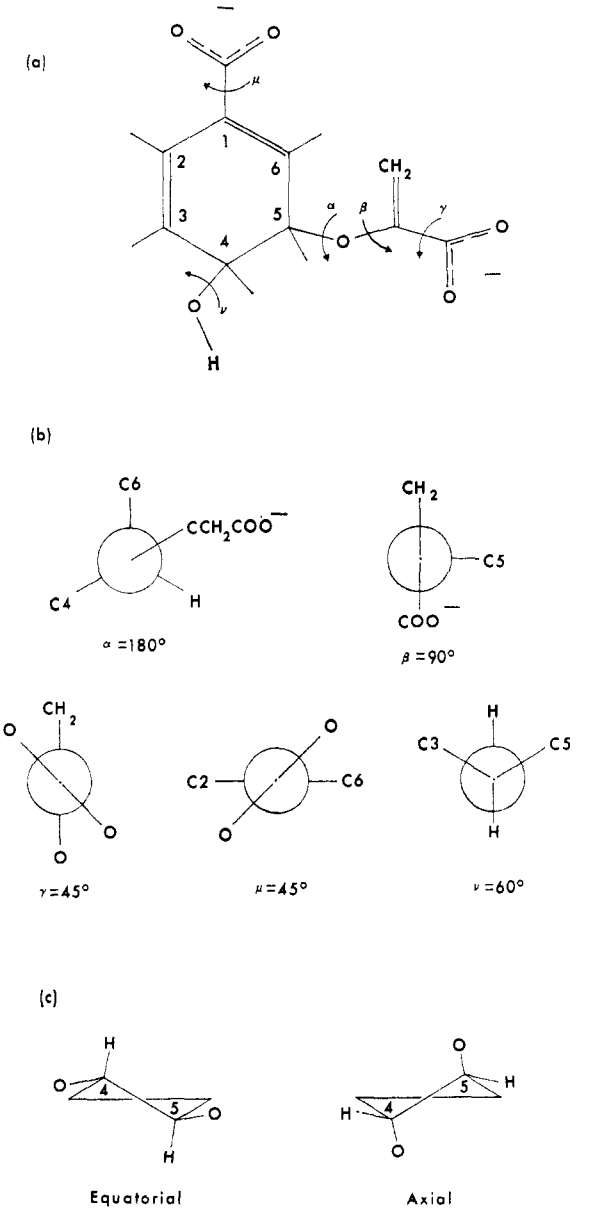

FIGURE 4: The six degrees of conformational freedom considered for chorismate. Part a gives the structure of chorismate and locates the five rotations which are defined by Newman projections in part b. In these projections the angles given correspond to clockwise rotations of the atoms below the plane of the page. Part c illustrates the two alternative conformations of the cyclohexadiene ring.

As a check of the validity of eq 2 and 3, and the reaction scheme (1), concentration *vs.* time curves were simulated at each temperature and compared with the experimental results. The solid lines in Figure 1 are representative of such simulated curves.

Figure 3 shows the temperature dependence of k_1, given by transition-state theory as

$$k_1 = \frac{RT}{Nh} e^{\Delta S^{\ddagger}/R} e^{-\Delta H^{\ddagger}/RT} \qquad (4)$$

where $\Delta S^{\ddagger}$ and $\Delta H^{\ddagger}$ are the entropy and enthalpy of activation, R is the gas constant, h is Planck's constant, N is Avogadro's number, and T is the absolute temperature. From the slope and intercept of this plot $\Delta H^{\ddagger}$ and $\Delta S^{\ddagger}$ for the conversion of chorismate to prephenate were calculated to be 20.71 ± 0.35 kcal/mol and −12.85 ± 0.42 eu, respectively

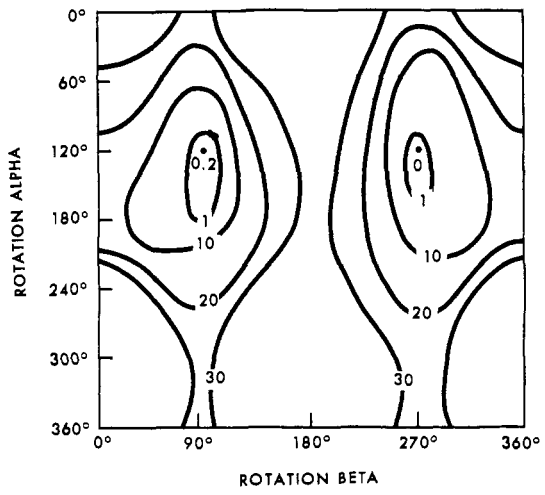

FIGURE 5: Contour map showing the effect of varying angles α and β (defined in Figure 4) on the calculated total energy (kcal/mol) of chorismate in the axial ring conformation.

(the corresponding parameters in the empirical Arrhenius treatment are 21.33 kcal/mol for the experimental energy of activation and 2.79×10^{10} for the frequency factor). For the reaction(s) described by k_3 the values of $\Delta H^{\ddagger}$ and $\Delta S^{\ddagger}$ were 23.57 ± 2.75 kcal/mol and -6.87 ± 1.48 eu.

Molecular Orbital Calculation Results. CHORISMATE. The structure of chorismate is given in Figure 4, where the six degrees of conformational freedom which have been considered for chorismate are also defined. Five of these are the rotations symbolized by α, β, γ, μ, and ν, and the sixth is the choice between the two "half-chair" forms of the cyclohexadiene ring, designated axial and equatorial in Figure 4 according to the positions of the major substituents on carbon atoms 4 and 5. The butadiene segment of the ring has been kept planar in both axial and equatorial conformations.

Three of these degrees of conformational freedom were expected to be of secondary importance, and were initially constrained to positions determined by the following considerations. In the absence of steric effects, the carboxyl groups involved in the rotations μ and γ are probably restrained by conjugation with neighboring groups to the regions $\mu = 0°$ ($\equiv 180°$) and $\gamma = 0°$ ($\equiv 180°$). The rotation ν, which is unlikely to have a strong intrinsic conformational preference, was fixed at $\nu = 60°$ where alterations to other conformational variables appeared least hindered sterically. The remaining rotations, α and β, were scanned from 0 to 360° for both ring conformations.

The results for the axial conformation are summarized in Figure 5, where it may be seen that two minima of approximately equal energy exist at $\alpha = 120°$ and $\beta = 90$ or 270°. Variation of γ, μ, and ν for these two conformations then led to $\gamma = 0°$, $\mu = 0°$, and $\nu = 60°$ as originally chosen. The energy barriers for rotations of β from 90 to 270° through 0° or 180° are 13 and 30 kcal/mol, respectively. These barriers reflect quite unfavorable interactions between the methylene or carboxyl groups and the chorismate ring. Rotation of α from 120 to 240–300° requires 28 kcal/mol at $\beta = 90°$ and 27 kcal/mol at $\beta = 270°$. Since the SNi′ mechanism proposed for the reaction by Edwards and Jackman (1965) involves α rotation in the axial conformation, these barriers provide a first indication of the energy in the transition state region, although no allowance has yet been made for changes in bond lengths and bond angles as the transition state is approached.

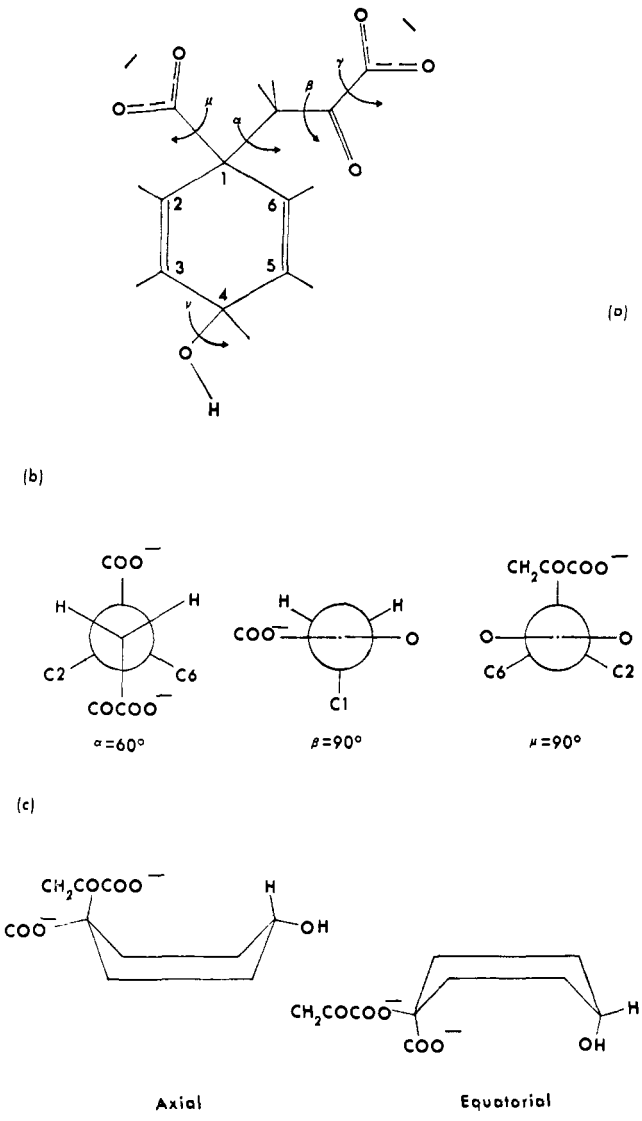

FIGURE 6: The six degrees of conformational freedom considered for prephenate. Part a gives the structure of prephenate and locates the rotations α, β, γ, μ, and ν. Of these, α, β, and μ are defined by Newman projections (using the same convention as Figure 4) in part b, while γ and ν are the rotations defined in Figure 4b. Part c illustrates the two alternative conformations of the cyclohexadiene ring.

Barriers to rotation for the minor variables γ, μ, and ν were 5.3, 1.5, and 1.2 kcal per mol, respectively.

For the equatorial conformation two minima recur at $\alpha = 120°$, $\beta = 90$ or 270°, and the best values of γ and μ are again those chosen initially, while for ν an angle of 300° lowers the total energy to 0.5 kcal/mol below that at $\nu = 60°$. The variation of energy with β is very similar to that shown for the axial form in Figure 5 but the barrier to α rotation is predictably smaller, being approximately 10 kcal/mol at $\beta = 90$ or 270°. The barriers for rotations γ, μ, and ν are effectively unchanged.

Comparison of the axial and equatorial energy distributions showed that all equatorial conformations were more stable than their axial counterparts, and the two minima are 7 kcal/mol lower in energy than the corresponding axial conformations. Additional calculations for a flat intermediate ring gave total energies of 6.5 and 6.6 kcal per mol (with respect to the equatorial minima) at $\alpha = 120°$, $\beta = 90$ and 270°, suggesting that no barrier separates the two ring forms.

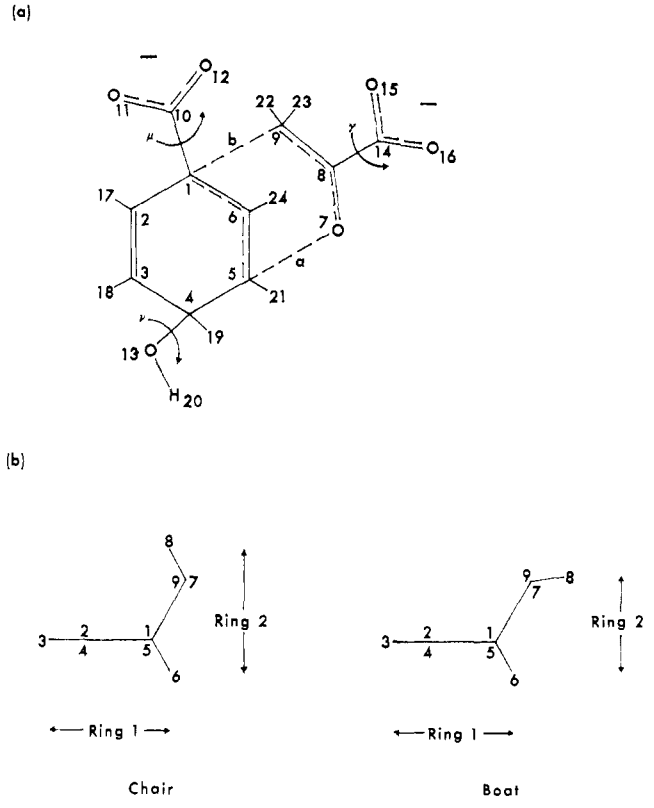

FIGURE 7: Part a gives the structure and atomic numbering of the transition state, and locates the rotations γ, μ, and ν, which are defined by the same Newman projections as the corresponding prephenate rotations (see Figures 4 and 6). Part b gives the two alternative ring conformations considered for the transition state.

However, the 7-kcal/mol difference in their energies indicates that less than one in a million chorismate molecules (Boltzmann distribution) is in the axial conformation at room temperature. This conclusion is in accord with the published nmr data of Edwards and Jackman (1965) who found that chorismate is equatorial in aqueous solution.

PREPHENATE. The prephenate structure is given in Figure 6,

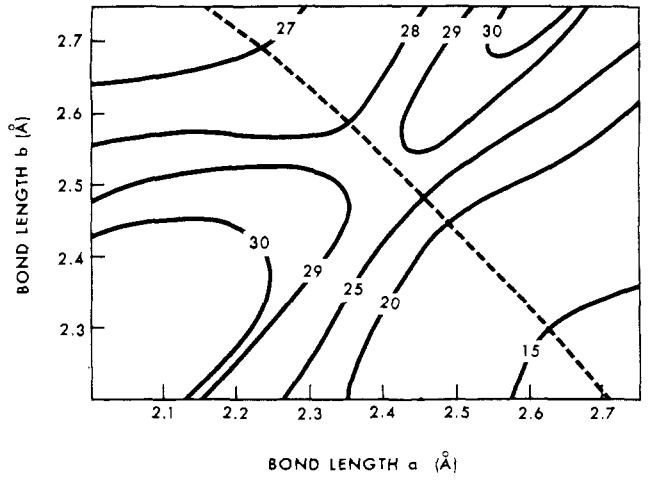

FIGURE 8: Contour map of the saddle-point region showing the effect of varying the bond lengths a and b (defined in Figure 7) on calculated total energy (kcal/mol). The transition state, which is the highest energy point on the lowest energy pathway, occurs at a = 2.4 Å and b = 2.5 Å. The reaction pathway (- - - - -) passes from the upper left to the lower right corner of the figure, and is given in elevation form in Figure 10.

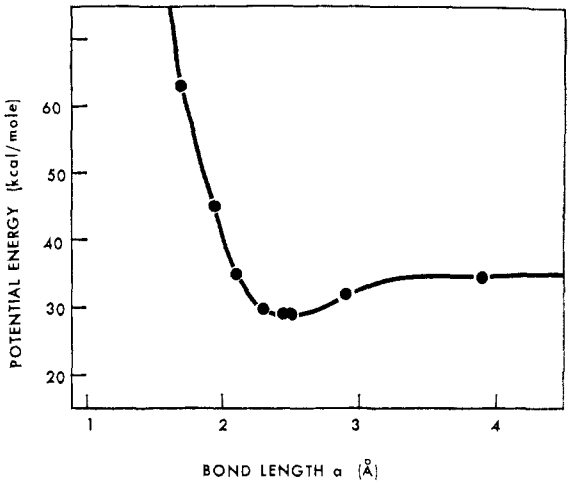

FIGURE 9: An elevation from Figure 8 depicting the energetics of dissociation of the transition state by simultaneously stretching bonds a and b, keeping $b = a + 0.1$ Å at each point. The potential energy values are relative to the most stable chorismate conformation.

and again six degrees of conformational freedom have been considered. Of these, the rotations γ and ν are those given in Figure 4, while rotations α, β, and μ are defined in Figure 6. The prephenate ring may exist in either of the two boat forms illustrated. They are designated axial and equatorial according to the positions of the pyruvyl group.

Rotations γ and ν were initially fixed ($\gamma = 0°$, $\nu = 300°$), and conformations with prohibitively short interatomic distances excluded. The molecular orbital calculations then provided a three-dimensional lattice (α, β, μ) of energies for each ring conformation. The most stable axial conformations had total energies 4 kcal/mol below the lowest energy equatorial conformations. The lowest energy conformation was axial with $\alpha = 60°$, $\beta = 30°$, $\gamma = 90°$, $\mu = 120°$, $\nu = 300°$ (or the mirror image angles) and had a total energy 1.5 kcal/mol lower than the most stable chorismate conformation. This is in accord with the effectively complete conversion of chorismate to prephenate observed chemically. The barriers to rotations α, β, γ, μ, and ν for the axial ring conformation were 14.2 (through 240°), *ca.* 5, 1.6, 0.9, and >1 kcal/mol, respectively, and similar values occur for the equatorial ring form.

TRANSITION STATE. The structure of the transition state is given in Figure 7. This simple two ring structure results directly from consideration of the reaction pathway, and particularly the need to incorporate partial bonds between C_5 and O_7, as in chorismate, and between C_1 and C_9, as in prephenate. The lengths of these bonds, designated a and b, respectively, in Figure 7, are two of the six degrees of conformational freedom considered for the molecule. The other four are the rotations γ, μ, and ν, defined as they were for prephenate, and the two alternative conformations for the second ring which are shown diagramatically in Figure 7. Initially the rotations were fixed at $\gamma = 0°$, $\mu = 0°$, and $\nu = 60°$ and the bond lengths were varied independently of each other for both ring conformations.

For the chair conformation the variation of total energy with the length of the incipient and excipient bonds in the saddle point region is given in Figure 8. Figure 9 is an elevation showing the effect on total energy of stretching both bonds simultaneously (keeping $b = a + 0.1$ Å) and Figure 10 (another elevation) depicts the lowest energy reaction pathway which is represented by the dashed line in Figure 8. The

TABLE II: Atomic Coordinates of the Atoms of the Transition State in Its Lowest Energy Conformation.

Atom[a]	Atomic Coordinates (Å)		
	X	Y	Z
1	0.000000	0.000000	0.000000
2	1.500000	0.000000	0.000000
3	2.200452	1.165748	0.000000
4	1.500094	2.482929	0.000000
5	0.000094	2.482928	0.000000
6	−0.507653	1.241507	0.716785
7	−0.801042	2.482928	−2.262340
8	−0.649936	1.332640	−2.952631
9	−0.834517	0.000000	−2.356604
10	−0.510724	−1.249018	0.721121
11	−1.227359	−2.046125	0.078039
12	−0.185872	−1.410045	1.917382
13	1.868497	3.215657	1.159219
14	−0.267175	1.391072	−4.432827
15	−0.642896	2.380792	−5.097499
16	0.402166	0.446176	−4.903629
17	2.041666	−0.957391	0.000000
18	3.300075	1.136953	0.000000
19	1.785476	3.050535	−0.897987
20	1.608909	2.700645	1.976150
21	−0.367094	3.380915	0.518453
22	−1.902371	−0.263740	−2.367987
23	−0.269140	−0.736584	−2.946344
24	−1.143454	1.242128	1.614424

[a] The numbering of the atoms is given in Figure 7.

highest point on the pathway, which corresponds to the transition state, is at a = 2.4 Å, b = 2.5 Å. Variation of the angles γ, μ, and ν for this basic conformation then gave the final transition-state structure, for which $\mu = 0°$, $\gamma = 30°$, $\nu = 60°$ and the total energy was 28.9 kcal/mol above the most stable chorismate conformation. This value is in good agreement with our experimental enthalpy of activation, 20.7 kcal/mol (see Discussion). The atomic coordinates of all the atoms in the transition state structure are given in Table II.

The saddle point for the boat form occurred at very similar bond lengths and rotation angles, but was 1.8 kcal/mol less stable than the chair form. Additional calculations for a flat intermediate structure gave a barrier of 7.5 kcal/mol for the conversion from the chair to boat conformation. Barriers to rotations γ, μ, and ν were 2.7, 1.1, and 1.2 kcal per mol, respectively, in the chair conformation.

Discussion

The primary function of an enzyme is to increase the rate at which biological substrates are transformed into their products. In the absence of enzyme, chorismate is converted to prephenate at pH 7.5 and 37° with a rate constant of 2.6×10^{-5} sec^{-1} (Table I). The enzyme chorismate mutase–prephenate dehydrogenase from *A. aerogenes* (EC 1.3.1.12) conforms to Michaelis–Menten kinetics with respect to its mutase reaction (Koch *et al.*, 1972) and we have calculated that its maximum velocity is 37.8 μmol/min per mg of protein. This calculation was made by extrapolation of the data in Figure 5 of Koch *et al.* (1972) and conversion into fundamental units (μmol/min per mg of protein) using the specific activity for the

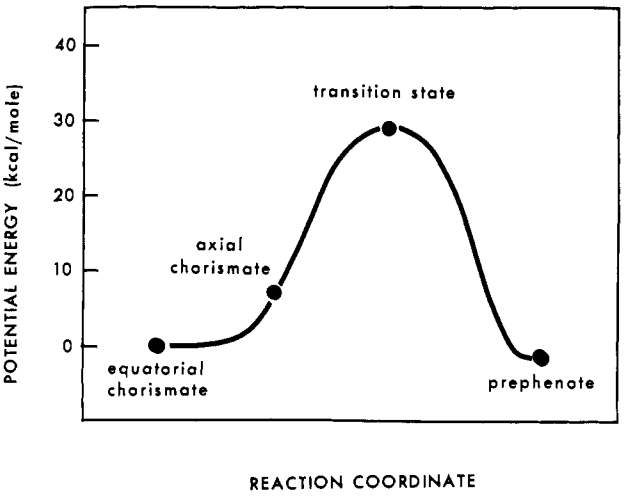

FIGURE 10: An elevation corresponding in part to the dashed line in Figure 8 and depicting the calculated lowest energy reaction pathway from chorismate anion in its most stable conformation to the lowest energy conformation of prephenate anion. The potential energy values are relative to the most stable chorismate conformation.

most highly purified enzyme (4200 "units"/mg) obtained by Koch *et al.* (1970), knowing that this corresponds to a chorismate concentration of 2.5 mM (see Methods in latter paper). The enzyme from *Escherichia coli*, although allosteric with respect to its mutase reaction, has a maximum velocity similar to this (Koch *et al.*, 1971). Assuming a single catalytic site per enzyme molecular weight of 80,000 (Koch *et al.*, 1970–1972) we have calculated a turnover number (molecules of substrate transformed per second per catalytic center) of 50.4 sec^{-1}, so that the rate of transformation to prephenate of enzyme-bound chorismate is 1.9×10^6 times that of free chorismate at pH 7.5 and 37°.

From eq 4 it may be seen that rate enhancement results from decreasing the enthalpy of activation and/or the entropy of activation. The measured nonenzymatic entropy of activation of −12.85 eu corresponds to the freezing of two internal rotations (denoted α and β in Figure 4) on passing from substrate to transition state. If these two rotations were to be similarly restricted on binding of the substrate by the enzyme, and the free rotations common to both substrate and transition state (γ, μ, and ν in Figure 4) were equally constrained by binding in both species, the entropy barrier would be reduced to zero, and the observed rate enhancement would require a reduction in the enthalpy of activation of only 4.9 kcal/mol. On the other hand, if rotation of the enolpyruvyl moiety were still free after enzyme binding the entropy of activation would remain −12.85 eu, and the observed rate enhancement would correspond to a reduction in the enthalpy of activation of 8.9 kcal/mol from the nonenzymatic value of 20.7 kcal/mol. It may thus be concluded that binding to the active site stabilizes the transition state by between 4.9 and 8.9 kcal per mol. The significance of this experimental result will be discussed further after considering the transition state structure predicted by the molecular orbital calculations.

The prediction of the transition state structure requires only qualitative use of the molecular orbital data in the saddle point region, since the corresponding enthalpy of activation has already been determined precisely by experiment. Nevertheless, this experimentally observed enthalpy of activation is within 25% of the value of 28.9 kcal/mol predicted for the transition state by our calculations, and any closer quantita-

tive agreement than this would certainly be considered fortuitous (Flurry, 1968), especially when the energies of two isomers with different hybridization states are being compared. Also, as indicated in the Results section, good qualitative agreement is again observed between the molecular orbital predictions and the two other experimental facts available, *i.e.*, that chorismate exists in the equatorial ring form (favored by 7 kcal/mol) and rearranges spontaneously to prephenate (favored by a further 1.5 kcal/mol). Comparison of theoretical and experimental findings thus provides good reason for confidence in the predicted transition-state structure. With the reasonable assumption that the enzyme-catalyzed reaction involves the same transition state, this structure reflects the active site of the enzyme, and we may now speculate concerning the nature of the bonds important for transition-state stabilization. Perhaps the most interesting features of the transition state are the positions of the hydroxyl, ring carboxyl (atoms 10, 11, and 12 in Figure 7) and side chain carboxyl (atoms 14, 15, and 16 in Figure 7) moieties, since these groups are all inherently capable of forming strong bonds with suitable partners. The most energetically favored positions for these groups may be seen in Table II, but it will be recalled that each group is subject to essentially free rotation, with barriers of 1.2 kcal/mol (hydroxyl), 1.1 kcal/mol (ring carboxyl), and 2.7 kcal/mol (side chain carboxyl). Each group may thus be considered to occupy a circular lamina of roughly 2 Å in diameter in a position defined by the transition-state ring structure and the bond lengths *a* and *b* (Figure 7). Bond formation from these regions to the active site could include ionic and reinforced ionic bonds from the carboxyl groups and hydrogen bonding to the hydroxyl moiety. However, although such a grouping of bonds could clearly account for the observed transition-state stabilization, it should be stressed that alternative bonding hypotheses could be advanced on the basis of the present data. It is therefore not feasible to specify the bonds stabilizing the transition state at this stage, but it is interesting to make some further use of the calculated potential energy surfaces to speculate on whether any other species on the reaction pathway, apart from the transition state, could be stabilized by the enzyme. For this to occur, the structure concerned would be likely to have several conformational properties in common with the transition state. One point on the calculated reaction pathway which obviously falls into this category is the axial form of chorismate, which, in common with the transition state, has the ring carboxyl and hydroxyl groups separated by *ca.* 5.5 Å, as opposed to *ca.* 6.4 Å in either equatorial chorismate or prephenate. It might thus be postulated that the activity of the enzyme involves binding to these two groups with an optimum separation of 5.5 Å, thus stabilizing the axial ring form and the transition state with respect to the initial equatorial chorismate conformation. Indeed, the calculated 7-kcal/mol difference between the equatorial and axial forms could readily be overcome by bonding to these two groups, so that this mechanism alone would be sufficient to account for the observed activity of the enzyme. Such a stabilization of an energetically less favored conformation has been referred to as substrate strain or distortion (Jencks, 1969). It is of interest in this regard that lysozyme has been postulated to act in part by stabilizing the half-chair conformation of one of the hexose rings in the substrate (Jencks, 1969). However, other equally attractive hypotheses could again be advanced, and tests to distinguish between them will require the use of substrate and transition-state analogs, and perhaps enzyme modification studies. As investigations (Koch *et al.*, 1972) aimed at identifying the amino acid residues present in the active site proceed, it should also become possible to identify the bonds which stabilize the transition state and thereby catalyze the reaction.

References

Allen, L. C., and Russell, J. D. (1967), *J. Phys. Chem. 46*, 1029.

Andrews, P. R. (1969), *J. Med. Chem. 12*, 761.

Blyholder, G., and Coulson, C. A. (1968), *Theor. Chim. Acta 10*, 316.

Dafforn, A., and Koshland, D. E. (1971), *Proc. Nat. Acad. Sci. U. S. 68*, 2463.

Edwards, J. M., and Jackman, L. M. (1965), *Aust. J. Chem. 18*, 1227.

Egan, A. F., and Gibson, F. (1972), *Biochem. J. 130*, 847.

Flurry, R. L. (1968), Molecular Orbital Theories of Bonding in Organic Molecules, London, Edward Arnold.

Gibson, F. (1970), *Methods Enzymol. 17A*, 362.

Gibson, F., and Pittard, J. (1968), *Bacteriol. Rev. 32*, 465.

Gibson, M. I., and Gibson, F. (1964), *Biochem. J. 90*, 248.

Gilvarg, C. (1955), *in* Amino Acid Metabolism, McElroy, W. D., and Glass, H. B., Ed., Baltimore, Md., Johns Hopkins Press, p 812.

Glasstone, S., and Lewis, D. (1961), Elements of Physical Chemistry, London, McMillan.

Hoffman, R. (1963), *J. Chem. Phys. 39*, 1397.

Jencks, W. P. (1969), Catalysis in Chemistry and Enzymology, New York, N. Y., McGraw-Hill.

Kier, L. B. (1972), Molecular Orbital Theory in Drug Research, New York, N. Y., Academic Press.

Koch, G. L. E., Shaw, D. C., and Gibson, F. (1970), *Biochim. Biophys. Acta 212*, 375.

Koch, G. L. E., Shaw, D. C., and Gibson, F. (1971), *Biochim. Biophys. Acta 229*, 795.

Koch, G. L. E., Shaw, D. C., and Gibson, F. (1972), *Biochim. Biophys. Acta 258*, 719.

Page, M. I. (1972), *Biochem. Biophys. Res. Commun. 49*, 940.

Page, M. I., and Jencks, W. P. (1971), *Proc. Nat. Acad. Sci. U. S. 68*, 1678.

Sutton, L. E. (1965), Tables of Interatomic Distances, Special Publication No. 11 and 18, The Chemical Society, London, and references therein.

Young, I. G., Gibson, F., and MacDonald, C. G. (1969), *Biochim. Biophys. Acta 192*, 62.